Multiple learning backtracking search algorithm for estimating parameters of photovoltaic models

Kunjie Yu[a,b], J.J. Liang[a,*], B.Y. Qu[c], Zhiping Cheng[a], Heshan Wang[a]

[a] School of Electrical Engineering, Zhengzhou University, Zhengzhou 450001, China
[b] Key Laboratory of Advanced Control and Optimization for Chemical Processes, Ministry of Education, East China University of Science and Technology, Shanghai 200237, China
[c] School of Electric and Information Engineering, Zhongyuan University of Technology, Zhengzhou 450007, China

HIGHLIGHTS

- MLBSA is proposed to identify the parameters of PV models.
- Multiple learning strategy aims to balance exploration and exploitation abilities.
- Elite method based on chaotic local search is used to refine population quality.
- Comprehensive experimental results indicate the competitive performance of MLBSA.

ARTICLE INFO

ABSTRACT

Obtaining appropriate parameters of photovoltaic models based on measured current-voltage data is crucial for the evaluation, control, and optimization of photovoltaic systems. Although many techniques have been developed to solve this problem, it is still challenging to identify the model parameters accurately and reliably. To improve parameters identification of different photovoltaic models, a multiple learning backtracking search algorithm (MLBSA) is proposed in this paper. In MLBSA, some individuals learn from the current population information and historical population information simultaneously, which aims to maintain population diversity and enhance the exploration ability. While other individuals learn from the best individual of current population to improve the convergence speed and thus enhance the exploitation ability. In addition, an elite strategy based on chaotic local search is developed to further refine the quality of current population. The proposed MLBSA is employed to solve the parameters identification problems of different photovoltaic models, i.e., single diode, double diode, and photovoltaic module. Comprehensive experimental results and analyses demonstrate that MLBSA outperforms other state-of-the-art algorithms in terms of accuracy, reliability, and computational efficiency.

1. Introduction

To solve the issues of climate change, environmental pollution, and depletion of classical fossil fuels, increasing attention has been focused on the using of renewable energy in recent years [1,2]. Among renewable energy sources, solar energy is regarded as one of the most promising renewable sources due to its wide availability and cleanliness [3–5]. It is converted into electricity and supply power through photovoltaic (PV) systems [6]. However, PV systems usually operate in harsh outdoor environment and their PV arrays are easy to be deteriorated, this greatly affects the utilization efficiency of solar energy [7]. Therefore, to control and optimize PV systems, it is very important

to evaluate the actual behavior of PV arrays in operation using accurate model based on measured current-voltage data [8]. Two steps are needed to model the PV models: (1) the mathematical model formulation, and (2) the model parameters identification [9,10]. Several mathematical models have been developed and proved to be successful in describing the performance and nonlinear behavior of PV systems [11]. Among them, the single diode model and double diode model are widely used in practice [12]. Furthermore, the accuracy of PV models primarily depends on their model parameters that usually are unavailable and varying due to aging, faults, and volatile operating conditions. Hence, accurately and reliably identify model parameters is indispensable to the evaluation, optimization, and control of PV

systems, and this motivates the development of various parameter identification methods over recent years [4,13,14].

The problem of estimating the PV models parameters is often defined as an optimization problem, and thus an objective function is necessary. Given that the measured current-voltage data involves a certain degree of noise, leading to the search space determined by the objective function is nonlinear and multimodal with multiple local optimal [15,16]. Some researchers have concentrated on using deterministic techniques, such as the least squares [17], the iterative curve fitting [18], and the tabular method [19], to solve the parameters identification problem. Since deterministic techniques generally are gradient-based methods, although these methods are powerful in local search, they are easy to be trapped in local optimal. In addition, the implementation of deterministic techniques requires numerous model restrictions such as convexity and differentiability, and many deterministic methods are highly sensitive to their initial solutions, which results in a lower efficiency when the initial point is far from the global optimal [15,20].

The heuristic methods inspired by various natural phenomena are a promising alternative to deterministic algorithms. They impose no restrictions on the problem formulation, thus can be easily used for various problems. Numerous heuristic methods and their variants have been proposed and used to estimate the PV models parameters in the past decade. Ishaque et al. [21] proposed a penalty based differential evolution (P-DE) to estimate the parameters of solar PV modules at varied environmental conditions. Muhsen et al. [3] developed a DE with integrated mutation (DEIM) for identifying the unknown parameters of double diode PV module model. Jiang et al. [22] developed an improved adaptive DE (IADE) based parameter identification approach by modifying the scaling factor and crossover rate. Askarzadeh and Rezazadeh [23] employed artificial bee swarm optimization (ABSO) to identify the solar cell parameters. Rajasekar et al. [24] used the bacterial foraging algorithm (BFA) to model the solar PV characteristics accurately. Niu et al. [15] put forward a simplified teaching–learning-based optimization (STLBO) to obtain the parameters of proton exchange membrane fuel and solar cells. Patel et al. [25] used TLBO to extract all the solar cell parameters from a single illuminated current-voltage data of different kinds of solar cells. Yuan et al. [26] developed a mutative-scale parallel chaos optimization algorithm (MPCOA) for solving the designed parameter estimation problem. Oliva et al. [27] applied artificial bee colony (ABC) to determine the parameters of solar cells accurately, and then they proposed an improved chaotic whale optimization algorithm (CWOA) for the same problems [9]. Askarzadeh and Coelho [28] simplified the bird mating optimizer (BMO) to extract the parameters of module model at different operation conditions. Ma et al. [29] compared and analyzed the performance of six bio-inspired optimization algorithms on the parameters estimation of single diode model. Chen et al. [30] studied the parameters estimation problem of solar cell models by using the proposed generalized oppositional TLBO (GOTLBO). Allam et al. [31] proposed month flame optimizer (MFO) for the parameters estimation of three diode model. Awadallah [32] designed five variants of BFA to estimate the parameters of PV module from nameplate data. Nunes et al. [1] proposed a guaranteed convergence particle swarm optimization (GCPSO) to determine the parameters of PV cells and modules. Jordehi [33] put forward a time varying acceleration coefficients PSO to estimate parameters of different PV models. Lin et al. [34] presented a modified simplified swarm optimization (MSSO) algorithm to extract the parameters of solar cell models. Chen et al. [35] developed a hybrid teaching-learning-based artificial bee colony (TLABC) for the solar PV parameters estimation problems. The results obtained by these heuristic algorithms are better than those found by deterministic methods considering robustness and accuracy. However, since the identification of PV models parameters is a multimodal problem containing many local optima, it is very difficult to achieve the global optimal solution for a considerable amount of heuristic algorithms. Furthermore, many

heuristic algorithms have several parameters need to be experimentally tuned, this affects their efficacy, accuracy, reliability, and scalability. Hence, looking for a competitive algorithm that can accurately and reliably identify the parameters of different PV models with satisfied computation time is still a challenging task.

Backtracking search algorithm (BSA) is a new population-based heuristic method proposed by Civicioglu for solving real-valued numerical optimization problems [36]. The algorithm has a simple structure and only one control parameter need to be set, and its performance is insensitive to the initial value of control parameter [37,38]. BSA has a memory pool that randomly maintains individuals of the previous generation population, which is used to generate the search-direction matrix by combining with the current population. Due to its flexibility and efficiency, BSA and its variants have been widely applied to a wide range of real-world optimization problems, such as economic dispatch problems [39,40], optimal power flow [41,42], parameter identification [43,44], feature selection [45], artificial neural network [46,47], community detection [48], flow shop scheduling [49,50], and nonlinear optimal control problem [51]. However, as a young algorithm, BSA has some disadvantages and its performance need to be further improved. The first is that only the historical population information is utilized to guide the search and the information in current population is not used sufficiently, which cannot maintain the population diversity efficiently and thus the exploration ability of BSA is weak. The second is that there is no guidance as approach to the current best individual during the evolution process, which leads to slow convergence speed and poor exploitation ability of BSA. In addition, to the best of our knowledge, no attempts to use BSA in handling the parameter identification problems of PV models have been reported in the literature.

The aim of this paper is to develop a multiple learning backtracking search algorithm (MLBSA) that has the capability to accurately and reliably extract the parameters of PV models with satisfied computation burden. In MLBSA, according to a random probability, some individuals update their positions by learning from the historical population information and current population information simultaneously, which can enhance the population diversity. While other individuals renew their positions guided by the best individual of current population to improve the convergence speed. In this way, the appropriate balance between the exploration and exploitation abilities can be achieved. Besides, to further refine the quality of current population, an elite mechanism based on chaotic local search is introduced. In order to evaluate the performance of MLBSA, it is compared with other state-of-the-art algorithms on parameters identification problems of different PV models, i.e., single diode, double diode, and PV module. Extensive experimental results and analyses indicate that MLBSA exhibits superior performance regarding accuracy and reliability with competitive computation efficiency.

The main contributions of this paper are as follows:

- A new method MLBSA is proposed to efficiently determine the parameters of PV models. In MLBSA, individuals randomly select different update equations for learning to balance the exploration and exploitation abilities.
- An elite mechanism based on chaotic local search is also developed to refine the quality of current population in each generation.
- The effectiveness of MLBSA is comprehensively tested through parameters identification problems of different PV models.

The remainder of this paper is organized as follows. Section 2 presents the problem formulation of PV models. Section 3 introduces the basic BSA algorithm. Section 4 presents the proposed MLBSA in detail. Section 5 displays the experimental results and analysis on different PV models. Finally, Section 6 concludes this paper.
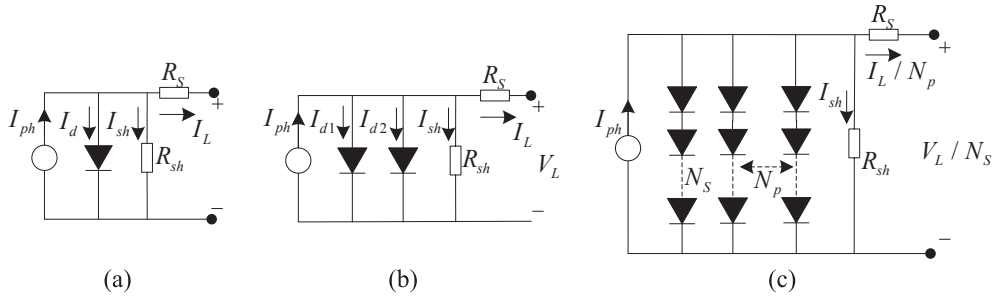
Fig. 1. Equivalent circuit diagrams for (a) single diode, (b) double diode, and (c) PV module.

2. Problem formulation

There exist several PV models that describe the current-voltage characteristics of the solar cells and PV modules in the literature. Among them, the single diode model and double diode model are the most commonly employed in practice. These two models and the objective function are presented as follows.

2.1. Solar cell model

2.1.1. Single diode model

Single diode model has been widely used to describe the static characteristic of solar cell due to its simplicity and accuracy. As shown in Fig. 1(a), this model consists of a current source in parallel to a diode, a shunt resistor to represent the leakage current, and a series resistor to account for losses related to load current. The output current is computed by Eq. (1).

$$I_L = I_{ph} - I_d - I_{sh} \tag{1}$$

where I_L denotes the terminal current (output current), I_{ph} represents the photo-generated current, I_d is the diode current obtained by Shockley Eq. (2), and I_{sh} is the shunt resistor current calculated by Eq. (3) [7,52].

$$I_d = I_{sd} \cdot \left[\exp\left(\frac{q \cdot (V_L + R_S \cdot I_L)}{n \cdot k \cdot T} \right) - 1 \right] \tag{2}$$

$$I_{sh} = \frac{V_L + R_S \cdot I_L}{R_{sh}} \tag{3}$$

where R_S and R_{sh} denote the series and shunt resistances, respectively. V_L represents the terminal voltage (output voltage), I_{sd} denotes the reverse saturation current of diode. n is the diode ideality factor, k is the Boltzmann constant ($1.3806503 \times 10^{-23}$ J/K), q is the magnitude of charge on an electron ($1.60217646 \times 10^{-19}$ C), and T is the cell temperature in Kelvin. Therefore, Eq. (1) can be rewritten as shown in Eq. (4).

$$I_L = I_{ph} - I_{sd} \cdot \left[\exp\left(\frac{q \cdot (V_L + R_S \cdot I_L)}{n \cdot k \cdot T} \right) - 1 \right] - \frac{V_L + R_S \cdot I_L}{R_{sh}} \tag{4}$$

From Eq. (4), it can be seen that the single diode model has five unknown parameters (I_{ph}, I_{sd} R_S R_{sh} n). Accurate estimation of these parameters is significant to reflect the solar cell performance, this can be achieved by an optimization method.

2.1.2. Double diode model

The single diode model ignores the effect of recombination current loss in the depletion region, when considering this loss, a more precise model namely double diode model is obtained [30]. This model has two diodes in parallel with the current source and a shunt resistance to shunt the photo-generated current source. One is set as a rectifier and the other is used to model the charge recombination current and some non-idealities [9]. The equivalent circuit is presented in Fig. 1(b), and

the output current is calculated by Eq. (5).

$$\begin{aligned} I_L &= I_{ph} - I_{d1} - I_{d2} - I_{sh} \\ &= I_{ph} - I_{sd1} \cdot \left[\exp\left(\frac{q \cdot (V_L + R_S \cdot I_L)}{n_1 \cdot k \cdot T} \right) - 1 \right] - I_{sd2} \cdot \left[\exp\left(\frac{q \cdot (V_L + R_S \cdot I_L)}{n_2 \cdot k \cdot T} \right) - 1 \right] - \frac{V_L + R_S \cdot I_L}{R_{sh}} \end{aligned} \tag{5}$$

where I_{sd1} and I_{sd2} denote the diffusion and saturation currents, respectively. n_1 and n_2 represent the diffusion and recombination diode ideality factors, respectively. From Eq. (5), it can be observed that the double diode model involves seven unknown parameters (I_{ph}, I_{sd1} I_{sd2}, R_S R_{sh} n_1, n_2), they require identifying to obtain the actual behavior of solar cell.

2.2. PV module model

PV module model usually contains several solar cells connected in series and/or in parallel. Fig. 1(c) gives the equivalent circuit of single diode PV module, and the output current can be formulated by Eq. (6).

$$I_L/N_p = I_{ph} - I_{sd} \cdot \left[\exp\left(\frac{q \cdot (V_L/N_S + R_S \cdot I_L/N_p)}{n \cdot k \cdot T} \right) - 1 \right] - \frac{V_L/N_S + R_S \cdot I_L/N_p}{R_{sh}} \tag{6}$$

where N_p and N_S denote the number of solar cells in parallel and series, respectively. Same as to the abovementioned single diode model, five unknown parameters (I_{ph}, I_{sd} R_S R_{sh} n) need to be identified.

2.3. Objective function

For the parameter identification problem of PV models, the main purpose is to seek the most optimal values for unknown parameters so as to minimize the difference between the measured and calculated current data. The error function for each pair of measured and calculated current data point is given by Eqs. (7) and (8) for single diode model and double diode model, respectively. Then, the overall difference is quantified by the root mean square error (RMSE) defined by Eq. (9), which is commonly used as the objective function [3,15,16,20,30,53]. Hence, in this study, the optimization process concerns with minimizing the objective function RMSE($\mathbf{x}$) by adjusting the solution vector $\mathbf{x}$ at each generation.

$$\begin{cases} f_k(V_L, I_L, \mathbf{x}) = I_{ph} - I_{sd} \cdot \left[\exp\left(\frac{q \cdot (V_L + R_S \cdot I_L)}{n \cdot k \cdot T} \right) - 1 \right] - \frac{V_L + R_S \cdot I_L}{R_{sh}} - I_L \\ \mathbf{x} = \{I_{ph}, I_{sd}, R_S, R_{Sh}, n\} \end{cases} \tag{7}$$

$$\begin{cases} f_k(V_L, I_L, \mathbf{x}) = I_{ph} - I_{sd1} \cdot \left[\exp\left(\frac{q \cdot (V_L + R_S \cdot I_L)}{n_1 \cdot k \cdot T} \right) - 1 \right] - I_{sd2} \cdot \left[\exp\left(\frac{q \cdot (V_L + R_S \cdot I_L)}{n_2 \cdot k \cdot T} \right) - 1 \right] \\ \qquad\qquad - \frac{V_L + R_S \cdot I_L}{R_{sh}} - I_L \\ \mathbf{x} = \{I_{ph}, I_{sd1}, I_{sd2}, R_S, R_{Sh}, n_1, n_2\} \end{cases} \tag{8}$$

$$RMSE(\mathbf{x}) = \sqrt{\frac{1}{N}\sum_{k=1}^{N}f_k(V_L, I_L, \mathbf{x})^2} \qquad (9)$$

where N is the number of experimental data and $k = 1, …, N$.

3. Backtracking search algorithm

BSA is a population-based intelligence optimization algorithm developed to be a global optimizer [36]. It has a simple structure and the history-related information plays an important role in its evolution process [46]. BSA involves two populations: current population and historical population. At the beginning of each generation, the historical population will be updated by randomly selecting from the historical and current populations. Then, a search-direction matrix is determined by these two populations to guide the search process. Since the historical population is used in BSA, a trail individual is generated by taking the partial advantage of the experiences from previous generations. The main idea behind BSA can be explained using five processes: initialization, selection-I, mutation, crossover, and selection-II. Herein, these processes are simply described and further details can be found in [36].

Step 1: Initialization. BSA randomly generates the initial population P and historical population $oldP$ using Eqs. (10) and (11), respectively.

$$P_{i,j} = low_j + rand \cdot (up_j - low_j) \qquad (10)$$

$$oldP_{i,j} = low_j + rand \cdot (up_j - low_j) \qquad (11)$$

where $i = 1, 2, …, NP$, and NP is the size of population. $j = 1, 2, …, D$, and D is the number of dimension of variables. low_j and up_j are the lower and upper boundaries on the jth variable, respectively. $rand$ is a uniformly distributed random number within [0, 1].

Step 2: Selection-I. At the beginning of each generation, $oldP$ is redefined through Eq. (12), and then the order of the individuals in $oldP$ is randomly changed by Eq. (13).

$$oldP = \begin{cases} P, & if(a < b | a, b \sim U(0, 1)) \\ oldP, & otherwise \end{cases} \qquad (12)$$

$$oldP = permuting(oldP) \qquad (13)$$

where a and b are two uniformly distributed random numbers between 0 and 1. = is the update operation, and $permuting$ function is a random shuffling function. Through Eq. (12), BSA can guarantee the designated population belongs to a randomly selected previous generation as the historical population that is remembered until it is changed.

Steps 3–4: Mutation and crossover. The mutant individuals are generated by the historical individuals and current individuals as shown in Eq. (14). Then, the crossover operator is conducted by Eq. (15). It can be seen that a binary integer-valued matrix (map) of size $NP \cdot D$ is used to guide the crossover direction. The value of map is controlled by the mix rate parameter that is the only control parameter should be determined in BSA, the details can be found in [36,47].

$$M = P + F \cdot (oldP - P) \qquad (14)$$

$$V_{i,j} = \begin{cases} P_{i,j}, & if \; map_{i,j} = 1 \\ M_{i,j}, & if \; map_{i,j} = 0 \end{cases} \qquad (15)$$

where F is a scale factor which controls the amplitude of the search-direction matrix, and its value is commonly set to $3 \cdot randn$, where $randn \sim N(0, 1)$. $V_{i,j}$ is the value of the jth variable for the ith trial individual.

Step 5: Selection-II. The greedy selection mechanism is used to form the new population P^{new}. As shown in Eq. (16), V_i is accepted if it provides a better function value than P_i considering the minimum problem.

$$P_i^{new} = \begin{cases} V_i, & if \; f(V_i) \leqslant f(P_i) \\ P_i, & otherwise \end{cases} \qquad (16)$$

Then, Steps 2–5 are continually performed until the termination criteria is satisfied to return the final solution.

4. Proposed multiple learning BSA (MLBSA)

4.1. Motivations

As mentioned above, the historical population is used in BSA and thus individuals update their positions by taking advantage of the experience from previous generations. This mechanism makes BSA is unique and efficient compared with other population-based algorithms that not use previous generations population. However, since the historical population is generated by randomly selecting from the past generations population and current population at the beginning of each iteration, this cannot ensure that the current population information is always extracted to form the historical population. As a result, individuals renew their positions only at the guidance of the previous generations population to some extent, this may lead to the population diversity quickly decrease if no strategy to improve it. In addition, the information from the best individual of current population is not considered, which makes BSA has slow convergence speed since individuals may be unable to rapidly locate the potential search region directed by the best individual. Moreover, although BSA has been successfully employed to deal with problems in different fields, as far as we know, there is no attempt of using BSA to solve the parameter estimation problem of PV models. Hence, based on these considerations, we propose the MLBSA to enhance the performance of BSA in estimating the parameters of PV models. To be specific, a multiple learning method is introduced to achieve the appropriate balance between the exploration and exploitation abilities, and an elite mechanism based on chaotic local search is proposed to further improve the quality of current population. The core idea behind MLBSA is elucidated as follows.

4.2. Multiple learning strategy

In the search process of BSA, the mutation operation plays a significant role in generating new individuals as shown in Eq. (14). However, only the historical population information is used to guide the search, and the current population information is not ensured to be used sufficiently at each generation. Thus, the population diversity and exploration ability of BSA are deteriorated quickly. Besides, the information about the best individual of current population is ignored, which is important to the convergence ability of BSA. Hence, to achieve a good balance between the exploration and exploitation abilities, a multiple learning strategy is introduced to replace the mutation and crossover operations of BSA for updating individuals' positions. Specifically, according to a random probability, some individuals learn from the historical population and current population simultaneously, while other individuals learn from the best individual of current population. The multiple learning method is used to generate new individual as shown in Eq. (17).

$$V_{i,j} = \begin{cases} P_{i,j} + F \cdot ((oldP_{i,j} - P_{i,j}) + (P_{h,j} - P_{i,j})), & if(a < b | a, b \sim U(0, 1)) \\ P_{i,j} + rand \cdot (P_{best,j} - P_{i,j}), & otherwise \end{cases} \qquad (17)$$

where h is an integer randomly selected from $\{1, 2, …, NP\}$ and satisfies $h \neq i$, so $P_{h,j}$ is the value of the jth variable for the individual h of current population. a and b are two uniformly distributed random numbers within [0, 1]. $P_{best,j}$ is the value of the jth variable for the best individual of current population.

Through the proposed multiple learning method, some individuals are devoted to improving the population diversity by both learning

from the historical population and current population, while other individuals are focused on enhancing the convergence speed via learning from the best individual in current population. Consequently, the performance of algorithm can be enhanced with both consideration of the exploration ability and exploitation ability.

4.3. Elite mechanism based on chaotic local search

During the whole evolution process, the current population is used to store the better individuals and considered to guide the search. As the exemplar, the quality of current population is very important and may affect the potential search directions. In this study, to further refine the quality of current population, an elite method based on chaotic local search is introduced. The local search aims to find the better solution around the current best solution. Considering chaotic sequence features randomicity and ergodicity, which is very beneficial to further improve the quality of one solution by generating new solution around it [15,20,54], so the well-known logistic map given by Eq. (18) is used in this study. In addition, it is expected that the best individual has more perturbations at the early stage to find the better individual. While at the latter stage, as the best individual is quite close to the global optimum, more information about the best individual should be retained. Hence, the chaotic local search presented in Eq. (19) is employed to generate a new individual V^* around the best individual. Then, the elite mechanism is performed to accept the new individual if it gives better function value than the worst one in current population. Therefore, the quality of current population can be refined through the elite mechanism based on chaotic local search at each generation.

$$z_{m+1} = 4 \cdot z_m \cdot (1 - z_m) \tag{18}$$

$$V_j^* = \begin{cases} P_{best,j} + rand_1 \cdot (2 \cdot z_m - 1), & \text{if } rand_2 < 1 - (FES/MaxFES) \\ P_{best,j}, & \text{otherwise} \end{cases} \tag{19}$$

where m is the iteration number, z_m is the value of mth chaotic iteration, and its initial value z_0 is randomly generated in [0, 1]. FES is the current number of function evaluations, and Max_FES is the maximum number of function evaluations. $rand_1$ and $rand_2$ are random numbers in the range [0, 1].

4.4. Framework of MLBSA

Based on aforementioned descriptions, the pseudo code of MLBSA is summarized in Algorithm 1 and the flow diagram of MLBSA is shown in Fig. 2. It can be observed that the proposed MLBSA retains the simple structure as that of basic BSA. In addition, the crossover operation is replaced by multiple learning and thus no parameter needs to be tuned in MLBSA, that is, MLBSA is free from algorithm-specific parameter. For the computational complexity, compared with the original BSA, the additional complexity of MLBSA derives from the multiple learning and elite mechanism based on chaotic local search. $O(NP-1)$ comparisons are needed to find the best individual in the multiple learning. $O(2 \cdot (NP-1))$ comparisons are performed for obtaining the best and worst individuals in the elite mechanism, and $O(D)$ is needed to implement the chaotic local search. Since the complexity of original BSA is $O(G_{max} \cdot NP \cdot D)$, where G_{max} is the maximal number of generation, the total complexity of MLBSA is $O(G_{max} \cdot (NP \cdot D + D + 3 \cdot (NP-1)))$. Thus, the proposed MLBSA does not significantly increase the overall complexity of the original BSA.

Algorithm 1. Pseudo code of MLBSA

1. Initialize population size and maximum number of function evaluations;
2. Initialize the current and historical populations using Eqs. (10) and (11), respectively;
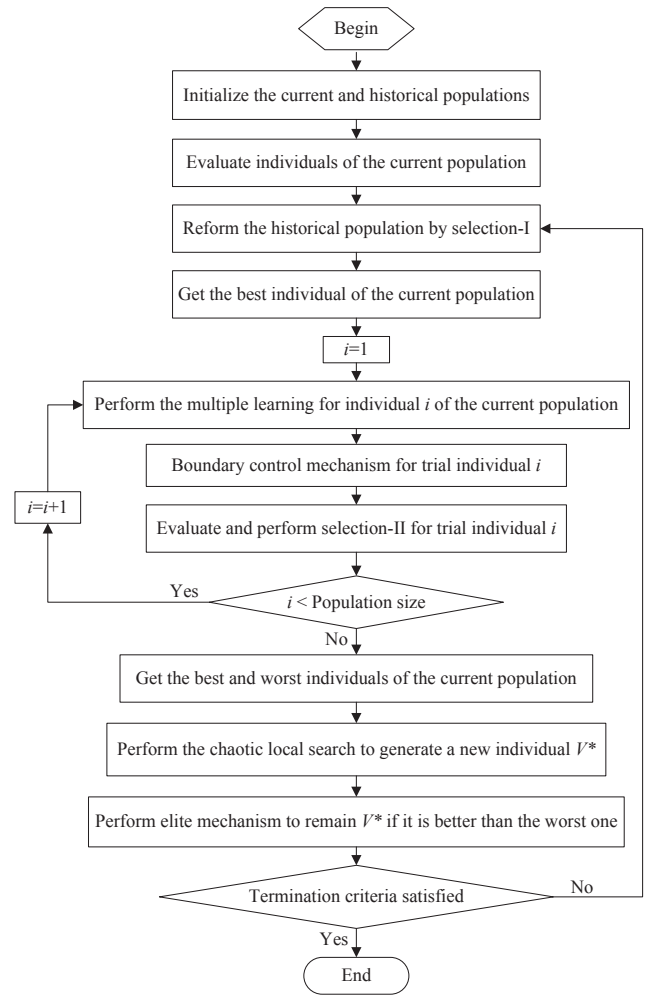3. Evaluate all individuals in the current population;

Fig. 2. The flow chart of MLBSA.

4. $FES = NP$;
5. **While** $FES < Max\_FES$ **do**
6.   Perform selection-I using Eqs. (12) and (13) to form the historical population;
7.   Find the best individual from the current population;
8.   **For** $i = 1$ to NP **do**
9.   Perform the multiple learning using Eq. (17) to generate the trial individual V_i;
10.   **For** $j = 1$ to D **do**   //*Boundary control mechanism *//
11.   **If** $(V_{i,j} < low_j)$ or $(V_{i,j} > up_j)$ **then**
        $V_{i,j} = low_j + rand \cdot (up_j - low_j)$ **End if**
12.   **End for**
13.   Evaluate the trial individual V_i;
14. $FES = FES + 1$;
15.   Implement selection-II using Eq. (16) to remain the better individual;
16.   **End for**
17.   Find the best and worst individuals from the current population;
18.   Implement the chaotic local search using Eq. (19) to generate a new individual V^*;
19.   Evaluate the new individual V^*;
20. $FES = FES + 1$;
21.   Perform the elite mechanism to accept V^* if it is better than the worst individual;
22. **End while**

Table 1
Parameters bounds of different PV models.

Parameter	Single diode/double diode		PV module	
	Lower bound	Upper bound	Lower bound	Upper bound
$I_{ph}(A)$	0	1	0	2
$I_{sd}, I_{sd1}, I_{sd2}(\mu A)$	0	1	0	50
$R_S(\Omega)$	0	0.5	0	2
$R_{sh}(\Omega)$	0	100	0	2000
n, n_1, n_2	1	2	1	50

5. Experimental results and analysis

In this section, to verify the effectiveness of the proposed MLBSA, it is evaluated on parameters identification of different PV models, i.e., single diode, double diode, and PV module. The benchmark experimental current-voltage data of a solar cell and a solar module are considered to compare with other well-established algorithms. The data are acquired from [17], where a 57 mm diameter commercial R.T.C. France silicon solar cell operating at an irradiance of 1000 W/m^2 and a temperature of 33 °C, and a solar module named Photowatt-PWP201 contains 36 polycrystalline silicon cells in series operating at an irradiance of 1000 W/m^2 and a temperature of 45 °C. The experimental data set has been commonly selected to test different methods designed for parameters estimation of PV models [7,15,20,26,27,30,55]. To make straight comparison, the lower and upper boundaries for each parameter are kept the same as those used in previous literatures and given in Table 1.

In order to validate the competitive performance of MLBSA, it is intensively compared with other eleven state-of-the-art algorithms. They are the basic BSA [36] and its three variants namely improved BSA (IBSA) [56], learning BSA (LBSA) [47], and oppositional BSA (OBSA) [43]; three TLBO variants including generalized oppositional TLBO (GOTLBO) [30], simplified TLBO (STLBO) [15], and TLBO with learning experience of other learners (LETLBO) [57]; two PSO variants namely comprehensive learning PSO (CLPSO) [58] and biogeography-based learning PSO (BLPSO) [59]; two hybrid algorithms involving DE with biogeography-based optimization (DE/BBO) [60] and DE/BBO with covariance matrix based migration (CMM-DE/BBO) [61]. According to the suggestions in the corresponding literatures, the parameter settings for all selected algorithms are presented in Table 2. All of the algorithms have the same maximum number of function evaluations (*Max_FES*) 50,000 in each run for each problem to achieve straight comparison. In addition, each algorithm is performed 30 times independently on every problem to record the statistical results.

Firstly, the statistical results and convergence performance are

Table 2
Parameter settings of the compared algorithms.

Algorithm	Parameters
MLBSA	$NP = 50$
IBSA	$NP = 50$, mix rate = $0.5(1 + \text{rand})$
LBSA	$NP = 50$, mix rate = 1
OBSA	$NP = 50$, mix rate = 1
BSA	$NP = 50$, mix rate = 1
GOTLBO	$NP = 50$, jumping rate $Jr = 0.3$
STLBO	$NP = 20$
LETLBO	$NP = 50$
CLPSO	$NP = 40$, inertia weight w: 0.9–0.2, acceleration coefficient $c = 1.49445$, refreshing gap $m = 5$
BLPSO	$NP = 40$, inertia weight w: 0.9–0.2, acceleration coefficient $c = 1.49445$, $I = E = 1$
DE/BBO	$NP = 100$, $I = E = 1$, $\pi_{\max} = 0.005$, $K = 2$, $F = \text{rand}(0.1,1)$, $CR = 0.9$
CMM-DE/BBO	$NP = 100$, $I = E = 1$, $\pi_{\max} = 0.005$, $K = 2$, $F = \text{rand}(0.1,1)$, $CR = 0.9$, $P_e = 0.5$

comprehensively analyzed and shown to compare the accuracy, robustness, and convergence speed of each algorithm. Then, comparisons are carried out based on the best RMSE values found by different methods in 30 runs. In the following subsections, to make comparisons clear, the overall best and the second best RMSE values among all algorithms are highlighted in **gray boldface** and **boldface**, respectively.

5.1. Comparisons on the statistical results and convergence performance

In this subsection, the accuracy, reliability, and convergence performance of different algorithms are evaluated by means of the statistical results and convergence graphs. Table 3 presents the statistical results of all involved algorithms in 30 independent runs. The minimum RMSE values reflect the accuracy, the mean RMSE values indicate the average accuracy, and SD is the standard deviation of RMSE and reflect the reliability of the estimated parameters. In addition, to identify the significant differences between MLBSA and its competitors, the Wilcoxon signed-rank test at 5% significant level is carried out [62]. "+"and "≈" in Table 3 indicate the MLBSA is significantly better than or similar to its competitor, respectively.

From Table 3, it is obvious that the proposed MLBSA outperforms other eleven algorithms on all three models in terms of the average accuracy and reliability. On single diode model, STLBO features the second best results regarding the average accuracy and reliability. On double diode model, the second best performance regarding the average accuracy is achieved by STLBO, while the second best result in terms of reliability is obtained by GOTLBO. On PV module model, the second best results in terms of average accuracy and reliability are both achieved by CMM-DE/BBO. Furthermore, from the results of Wilcoxon signed-rank test shown in the last column of Table 3, it can be observed that MLBSA performs significantly better than its all competitors both on single diode model and double diode model. On PV module model, although the result of MLBSA is no significant difference with that of CMM-DE/BBO, it also significantly outperforms the remaining ten algorithms.

In addition, Fig. 3 gives the boxplots to show the distribution of results found by different algorithms in 30 independent runs. Note that the symbol "+" in Fig. 3 denote the outlier when plotting the boxplot. The comparisons on the span of the solution distribution also demonstrate the outstanding performance of the proposed MLBSA in contrast with other algorithms in terms of accuracy and reliability.

In order to investigate the computational efficiency of MLBSA, the mean computational time of all the selected algorithms on three models are recorded. The CPU time for each algorithm in the 30 runs are obtained on a PC Intel Core 3 Duo 3.30 GHz with a 4 GB RAM that runs on Windows 7 with MATLAB R2014a implementation. The results are illustrated in Fig. 4. As shown in Fig. 4, on each model, LETLBO consumes a longer computational time compared with the other algorithms, while OBSA requires the lowest computational overhead among all algorithms. MLBSA also features competitive performance since it needs a less computational time than most of the other algorithms on each model. This implies that the proposed algorithm can obtain the superior results with fairly satisfactory computational efficiency.

Fig. 5 presents the convergence curves of different algorithms to indicate the average RMSE performance of the 30 independent runs. It is obvious that MLBSA has the faster convergence speed than most of the other algorithms, especially on single diode model and double diode model.

The above extensive comparisons demonstrate that MLBSA features better searching accuracy, reliability, and faster convergence speed when estimating the parameters of different PV models, and its performance is superior or competitive compared with other well-established algorithms.

Table 3
Comparisons on the statistical results of different algorithms for three models.

Model	Algorithm	RMSE				Sig.
		Min	Mean	Max	SD	
Single diode model	MLBSA	**9.8602E-04**	**9.8602E-04**	**9.8602E-04**	**9.1461E-12**	
	IBSA	1.0092E-03	1.3198E-03	1.6235E-03	1.4509E-04	+
	LBSA	1.0143E-03	1.2370E-03	1.5890E-03	1.5895E-04	+
	OBSA	9.8602E-04	1.4579E-03	2.6561E-03	4.6196E-04	+
	BSA	1.0398E-03	2.5674E-03	3.8151E-02	6.7220E-03	+
	GOTLBO	9.8856E-04	1.0450E-03	1.2067E-03	5.0218E-05	+
	STLBO	9.8602E-04	**9.8607E-04**	**9.8655E-04**	**1.2438E-07**	+
	LETLBO	9.8738E-04	1.0333E-03	1.1593E-03	4.6946E-05	+
	CLPSO	9.9633E-04	1.0581E-03	1.3196E-03	7.4854E-05	+
	BLPSO	1.0272E-03	1.3139E-03	1.7928E-03	2.1166E-04	+
	DE/BBO	9.9922E-04	1.2948E-03	2.2258E-03	2.5074E-04	+
	CMM-DE/BBO	**9.8605E-04**	1.0486E-03	1.3475E-03	8.1679E-05	+
Double diode model	MLBSA	**9.8249E-04**	**9.8518E-04**	**9.8798E-04**	**1.3482E-06**	
	IBSA	9.9663E-04	1.5380E-03	2.5627E-03	4.0899E-04	+
	LBSA	1.0165E-03	1.2728E-03	1.7372E-03	1.8952E-04	+
	OBSA	1.0114E-03	1.8047E-03	7.8002E-03	1.2287E-03	+
	BSA	1.0182E-03	1.4437E-03	2.0214E-03	2.5282E-04	+
	GOTLBO	9.8742E-04	1.1475E-03	**1.3947E-03**	**1.1330E-04**	+
	STLBO	**9.8252E-04**	**1.0585E-03**	2.4480E-03	2.8978E-04	+
	LETLBO	9.8565E-04	1.0869E-03	1.4870E-03	1.5360E-04	+
	CLPSO	9.9894E-04	1.1458E-03	1.5494E-03	1.4367E-04	+
	BLPSO	1.0628E-03	1.4821E-03	1.7411E-03	1.7789E-04	+
	DE/BBO	1.0255E-03	1.5571E-03	2.4042E-03	3.6297E-04	+
	CMM-DE/BBO	1.0088E-03	1.5487E-03	2.0589E-03	2.9413E-04	+
PV module model	MLBSA	**2.425075E-03**	**2.425084E-03**	**2.425312E-03**	**4.336794E-08**	
	IBSA	**2.425093E-03**	2.437017E-03	2.478180E-03	1.271344E-05	+
	LBSA	2.429630E-03	2.493072E-03	2.608134E-03	4.652857E-05	+
	OBSA	**2.425075E-03**	1.452291E-02	3.316020E-01	6.013168E-02	+
	BSA	2.430121E-03	1.153909E-02	2.742508E-01	4.961834E-02	+
	GOTLBO	2.426583E-03	2.475386E-03	2.563849E-03	2.938836E-05	+
	STLBO	**2.425075E-03**	2.055293E-02	2.742508E-01	6.896273E-02	+
	LETLBO	2.425116E-03	2.440659E-03	2.582052E-03	2.949002E-05	+
	CLPSO	2.428064E-03	2.454903E-03	2.543269E-03	2.580951E-05	+
	BLPSO	2.425236E-03	2.437873E-03	2.488348E-03	1.372409E-05	+
	DE/BBO	2.428255E-03	2.461623E-03	2.525560E-03	2.925123E-05	+
	CMM-DE/BBO	**2.425075E-03**	**2.425175E-03**	**2.426796E-03**	**3.554783E-07**	≈

5.2. Comparisons on the detailed results

In this subsection, the best RMSE and the related parameters esti-mated by different algorithms are compared in detail.

5.2.1. Results on the single diode model

For single diode model, Table 4 gives the comparison results

including the estimated five parameters and RMSE values. It can be observed from Table 4 that MLBSA, together with OBSA and STLBO, achieve the best RMSE value (9.8602E−04) among all compared al-gorithms. While CMM-DE/BBO obtains the second best RMSE value (9.8605E−04), followed by LETLBO, GOTLBO, CLPSO, DE/BBO, IBSA, LBSA, BLPSO, and BSA. Since information about the accurate para-meters values is unavailable, the RMSE is used to indicate the accuracy.
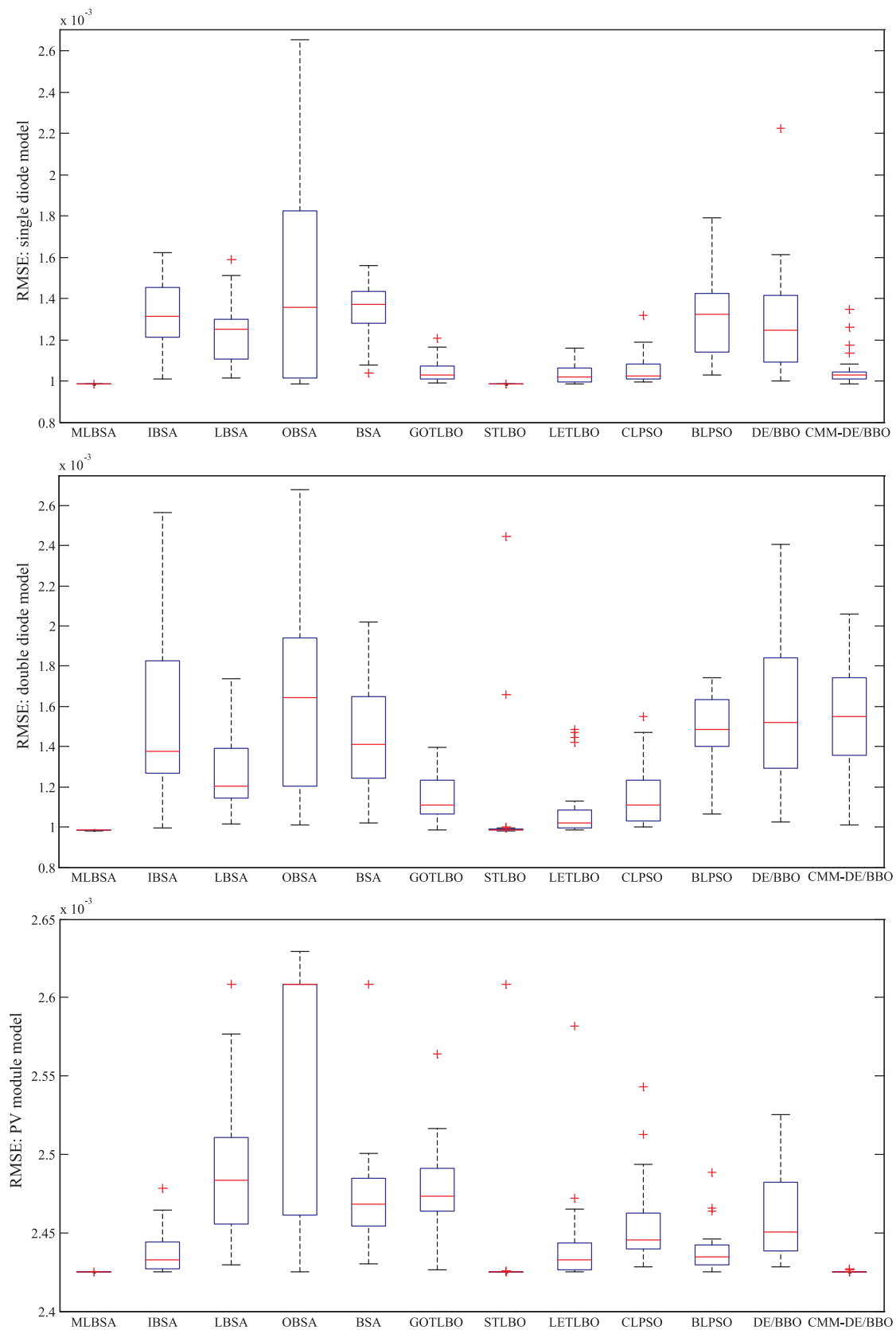
Fig. 3. Best RMSE boxplot in 30 runs of different algorithms for three models.

Although the RMSE values found by other algorithms except OBSA and STLBO are close to that obtained by MLBSA, any decrease on the objective function is significant as it makes improvement in the

knowledge on the actual parameters values. In order to further show the quality of the results, the individual absolute errors (IAE) in terms of current and power between the experimental data and simulated
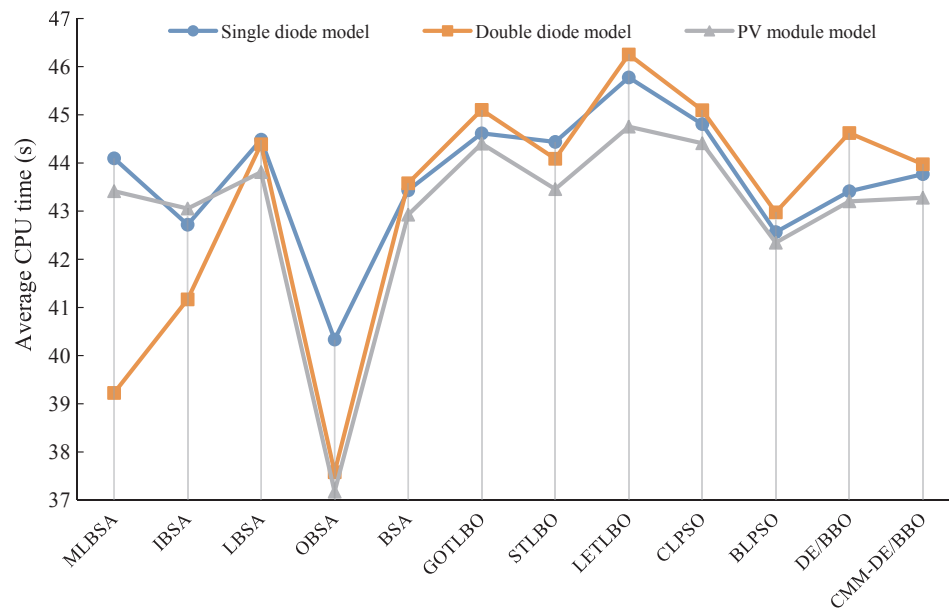
Fig. 4. The average CPU time of different algorithms for three models.

data are given in Table 5. All IAE values on current are less than 2.51E−03 and those on power are not more than1.46E−03, which confirm the accuracy of the estimated parameters. In addition, the best parameters extracted by MLBSA are employed to generate the *I-V* and *P-V* curves. As shown in Fig. 6, it is clear that the simulated data obtained

by MLBSA are highly in coincidence with the experimental data over the whole voltage range.

5.2.2. Results on the double diode model

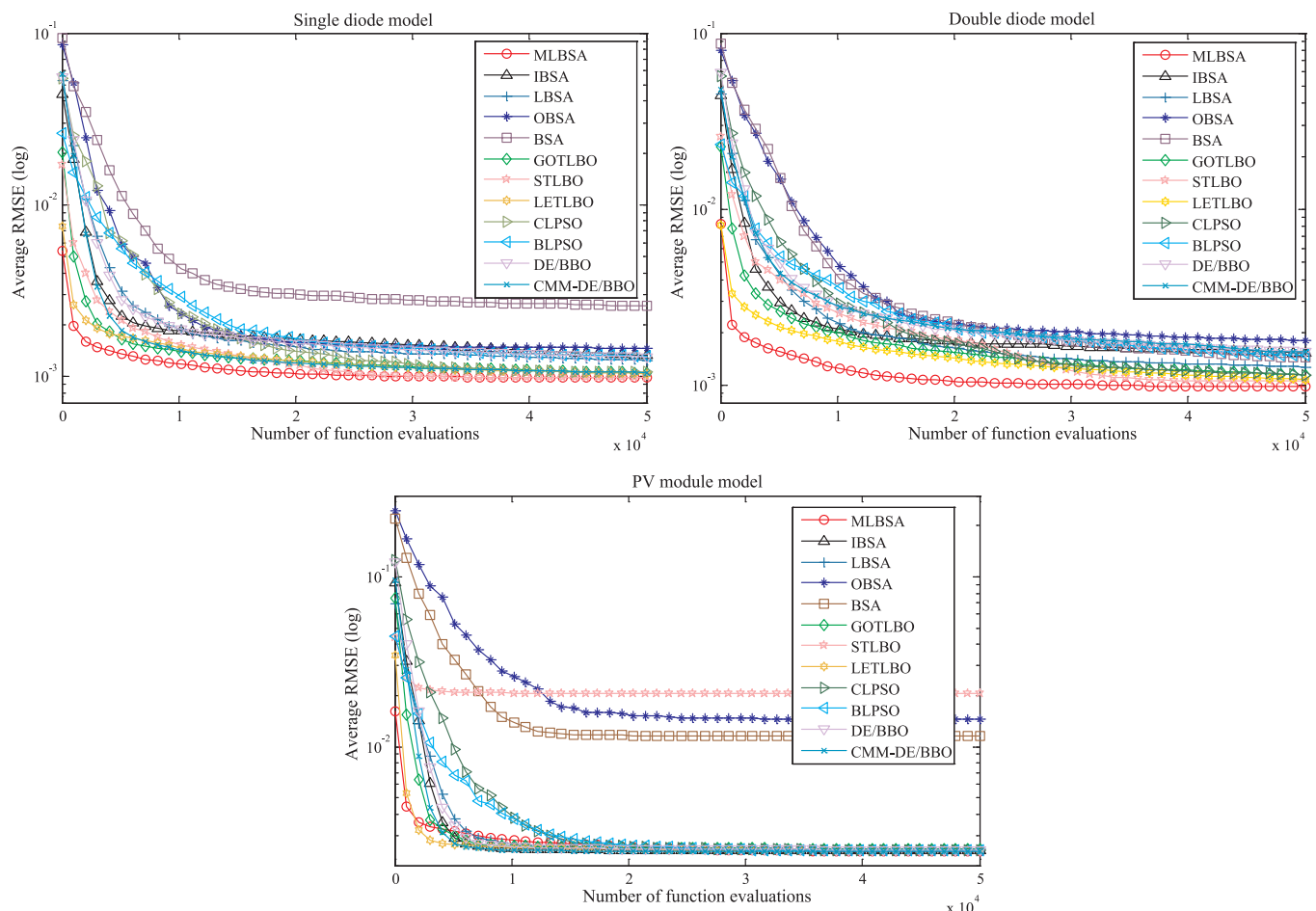For double diode model, Table 6 lists the estimated seven

Fig. 5. Convergence graphs of different algorithms for three models.

Table 4
Comparison among different algorithms on single diode model.

Algorithm	I_{ph}(A)	I_{sd}(μA)	R_S(Ω)	R_{sh}(Ω)	n	RMSE
MLBSA	0.7608	0.32302	0.0364	53.7185	1.4812	**9.8602E-04**
IBSA	0.7607	0.35502	0.0361	58.2012	1.4907	1.0092E-03
LBSA	0.7606	0.34618	0.0362	59.0978	1.4881	1.0143E-03
OBSA	0.7608	0.32302	0.0364	53.7187	1.4812	**9.8602E-04**
BSA	0.7609	0.37749	0.0358	56.5266	1.4970	1.0398E-03
GOTLBO	0.7608	0.3297	0.0363	53.3664	1.4833	9.8856E-04
STLBO	0.7608	0.3230	0.0364	53.7184	1.4812	**9.8602E-04**
LETLBO	0.7608	0.32597	0.0363	53.7429	1.4821	9.8738E-04
CLPSO	0.7608	0.34302	0.0361	54.1965	1.4873	9.9633E-04
BLPSO	0.7607	0.36620	0.0359	60.2845	1.4939	1.0272E-03
DE/BBO	0.7605	0.32477	0.0364	55.2627	1.4817	9.9922E-04
CMM-DE/BBO	0.7608	0.32384	0.0364	53.8753	1.4814	**9.8605E-04**

Table 5
IAE of MLBSA on single diode model.

Item	Measured data		Simulated current data		Simulated power data	
	V (V)	I (A)	I_{sim} (A)	IAE_I (A)	P_{sim} (W)	IAE_P (W)
1	−0.2057	0.7640	0.764087704	0.00008770	−0.15717284	0.00001804
2	−0.1291	0.7620	0.762663086	0.00066309	−0.09845980	0.00008560
3	−0.0588	0.7605	0.761355307	0.00085531	−0.04476769	0.00005029
4	0.0057	0.7605	0.760153991	0.00034601	0.00433288	0.00000197
5	0.0646	0.7600	0.759055209	0.00094479	0.04903497	0.00006103
6	0.1185	0.7590	0.758042345	0.00095765	0.08982802	0.00011348
7	0.1678	0.7570	0.757091654	0.00009165	0.12703998	0.00001538
8	0.2132	0.7570	0.756141365	0.00085864	0.16120934	0.00018306
9	0.2545	0.7555	0.755086873	0.00041313	0.19216961	0.00010514
10	0.2924	0.7540	0.753663878	0.00033612	0.22037132	0.00009828
11	0.3269	0.7505	0.751390966	0.00089097	0.24562971	0.00029126
12	0.3585	0.7465	0.747353851	0.00085385	0.26792636	0.00030611
13	0.3873	0.7385	0.740117222	0.00161722	0.28664740	0.00062635
14	0.4137	0.7280	0.727382225	0.00061777	0.30091803	0.00025557
15	0.4373	0.7065	0.706972651	0.00047265	0.30915914	0.00020669
16	0.4590	0.6755	0.675280152	0.00021985	0.30995359	0.00010091
17	0.4784	0.6320	0.630758272	0.00124173	0.30175476	0.00059404
18	0.4960	0.5730	0.571928358	0.00107164	0.28367647	0.00053153
19	0.5119	0.4990	0.499607018	0.00060702	0.25574883	0.00031073
20	0.5265	0.4130	0.413648792	0.00064879	0.21778609	0.00034159
21	0.5398	0.3165	0.317510109	0.00101011	0.17139196	0.00054526
22	0.5521	0.2120	0.212154939	0.00015494	0.11713074	0.00008554
23	0.5633	0.1035	0.102251311	0.00124869	0.05759816	0.00070339
24	0.5736	−0.0100	−0.008717542	0.00128246	−0.00500038	0.00073562
25	0.5833	−0.1230	−0.125507413	0.00250741	−0.07320847	0.00146257
26	0.5900	−0.2100	−0.208472326	0.00152767	−0.12299867	0.00090133
Sum of IAE				0.02152687		0.00873078

parameters and RMSE values obtained by different algorithms. Among all involved algorithms, it can be seen that the proposed MLBSA gets the best RMSE value (9.8249E−04), and STLBO provides the second best result. In contrast, the rest of algorithms achieve the inferior RMSE values, especially the result found by BLPSO is the worst one. Table 7 gives the IAE values and Fig. 7 presents the *I-V* and *P-V* characteristics of the best model estimated by MLBSA and the experimental data. From Table 7, all IAE values in terms of current are smaller than 2.54E−03 and those in terms of power are less than 1.48E−03, which indicate that the high-accurately identified parameters are achieved by MLBSA. From Fig. 7, it is clear that the simulated data of MLBSA are in good agreement with the experimental data.

5.2.3. Results on the PV module model

For PV module model, there are five parameters require to be extracted. Table 8 shows the estimated parameters and RMSE values found by each algorithm. It can be seen that MLBSA, OBSA, STLBO, and CMM-DE/BBO obtain the best RMSE value (2.425075E−03) among all considered algorithms, while IBSA gets the second best RMSE value. This followed by LETLBO, BLPSO, GOTLBO, CLPSO, DE/BBO, LBSA, and BSA. In addition, the calculated data obtained by MLBSA and experimental data are compared in Table 9 and Fig. 8. Results show that high accuracy parameters are extracted again by MLBSA, since all the IAE values on current are not greater than 4.96E−03 and the *I-V* and *P-V* characteristics of the identified model are also in quite good agreement with the experimental data.
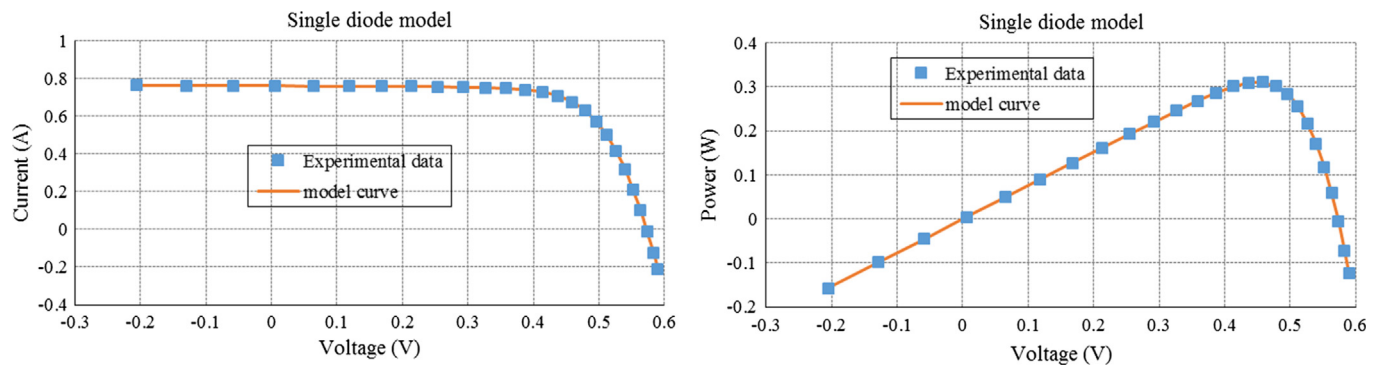
Fig. 6. Comparisons between the experimental data and simulated data obtained by MLBSA for single diode model: *I-V* and *P-V* characteristics.

Table 6
Comparison among different algorithms on double diode model.

Algorithm	I_{ph}(A)	I_{sd1}(µA)	R_S(Ω)	R_{sh}(Ω)	n_1	I_{sd2}(µA)	n_2	RMSE
MLBSA	0.7608	0.22728	0.0367	55.4612	1.4515	0.73835	2	**9.8249E-04**
IBSA	0.7608	0.21507	0.0366	51.9008	1.8718	0.26624	1.4651	9.9663E-04
LBSA	0.7606	0.29814	0.0363	60.1880	1.4760	0.27096	1.9202	1.0165E-03
OBSA	0.7608	0.17185	0.0372	54.5778	1.4313	0.42006	1.7759	1.0114E-03
BSA	0.7605	0.33210	0.0363	59.9671	1.8804	0.27694	1.4704	1.0183E-03
GOTLBO	0.7608	0.13894	0.0365	53.4058	1.7254	0.26209	1.4658	9.8742E-04
STLBO	0.7608	0.23364	0.0367	55.3382	1.4538	0.68494	2	**9.8252E-04**
LETLBO	0.7608	0.17390	0.0365	54.3021	1.6585	0.22664	1.4578	9.8565E-04
CLPSO	0.7607	0.25843	0.0367	57.9422	1.4625	0.38615	1.9435	9.9894E-04
BLPSO	0.7608	0.27189	0.0366	61.1345	1.4674	0.43505	1.9662	1.0628E-03

Table 7
IAE of MLBSA on double diode model.

| Item	Measured data		Simulated current data		Simulated power data	
	V (V)	I (A)	I_{sim} (A)	IAE_I (A)	P_{sim} (W)	IAE_P (W)
1	−0.2057	0.7640	0.76398479	0.00001521	−0.15715167	0.00000313
2	−0.1291	0.7620	0.76260487	0.00060487	−0.09845229	0.00007809
3	−0.0588	0.7605	0.76133792	0.00083792	−0.04476667	0.00004927
4	0.0057	0.7605	0.76017352	0.00032648	0.00433299	0.00000186
5	0.0646	0.7600	0.75910698	0.00089302	0.04903831	0.00005769
6	0.1185	0.7590	0.75812037	0.00087963	0.08983726	0.00010424
7	0.1678	0.7570	0.75718735	0.00018735	0.12705604	0.00003144
8	0.2132	0.7570	0.75624231	0.00075769	0.16123086	0.00016154
9	0.2545	0.7555	0.75517623	0.00032377	0.19219235	0.00008240
10	0.2924	0.7540	0.75372180	0.00027820	0.22038825	0.00008135
11	0.3269	0.7505	0.75139936	0.00089936	0.24563245	0.00029400
12	0.3585	0.7465	0.74730258	0.00080258	0.26790797	0.00028772
13	0.3873	0.7385	0.74001256	0.00151256	0.28660687	0.00058582
14	0.4137	0.7280	0.72724918	0.00075082	0.30086299	0.00031061
15	0.4373	0.7065	0.70685217	0.00035217	0.30910645	0.00015400
16	0.4590	0.6755	0.67521144	0.00028856	0.30992205	0.00013245
17	0.4784	0.6320	0.63076043	0.00123957	0.30175579	0.00059301
18	0.4960	0.5730	0.57199341	0.00100659	0.28370873	0.00049927
19	0.5119	0.4990	0.49970440	0.00070440	0.25579868	0.00036058
20	0.5265	0.4130	0.41373235	0.00073235	0.21783008	0.00038558
21	0.5398	0.3165	0.31754587	0.00104587	0.17141126	0.00056456
22	0.5521	0.2120	0.21212391	0.00012391	0.11711361	0.00006841
23	0.5633	0.1035	0.10216514	0.00133486	0.05754962	0.00075193
24	0.5736	−0.0100	−0.00879026	0.00120974	−0.00504209	0.00069391
25	0.5833	−0.1230	−0.12554285	0.00254285	−0.07322915	0.00148325
26	0.5900	−0.2100	−0.20837364	0.00162636	−0.12294044	0.00095956
Sum of IAE				0.02127670		0.00877565
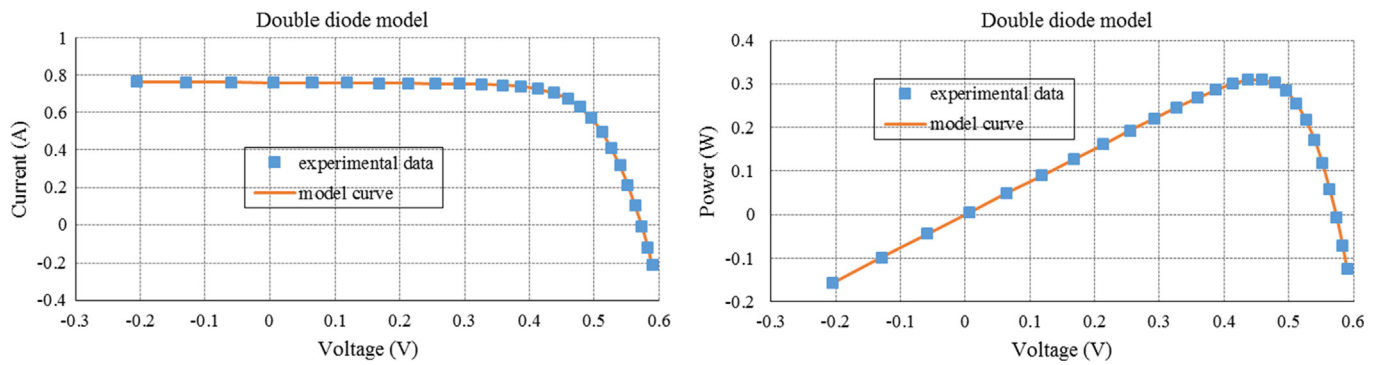
Fig. 7. Comparisons between the experimental data and simulated data obtained by MLBSA for double diode model: *I-V* and *P-V* characteristics.

Table 8
Comparison among different algorithms on PV module model.

Algorithm	I_{ph}(A)	I_{sd}(μA)	R_S(Ω)	R_{sh}(Ω)	n	RMSE
MLBSA	1.0305	3.4823	1.2013	981.9823	48.6428	**2.425075E-03**
IBSA	1.0305	3.4923	1.2010	986.7363	48.6537	**2.425093E-03**
LBSA	1.0304	3.5233	1.2014	1020.4	48.6866	2.429630E-03
OBSA	1.0305	3.4832	1.2012	982.1261	48.6439	**2.425075E-03**
BSA	1.0302	3.6483	1.1972	1050.7	48.8214	2.430120E-03
GOTLBO	1.0307	3.5124	1.1995	969.9313	48.6766	2.426583E-03
STLBO	1.0305	3.4824	1.2013	982.0387	48.6430	**2.425075E-03**
LETLBO	1.0306	3.4705	1.2015	974.6190	48.6301	2.425116E-03
CLPSO	1.0304	3.6131	1.1978	1017.0	48.7847	2.428064E-03
BLPSO	1.0305	3.5176	1.2002	992.7901	48.6815	2.425236E-03
DE/BBO	1.0303	3.6172	1.1969	1015.1	48.7894	2.428255E-03
CMM-DE/BBO	1.0305	3.4823	1.2013	981.9823	48.6428	**2.425075E-03**

5.3. Effectiveness of introduced mechanisms

In this subsection, some experiments are conducted to demonstrate the effectiveness of different introduced mechanisms in MLBSA. The parameter settings are kept the same as those in preceding experiments of this study. To this end, MLBSA employs the mutation and crossover strategy in basic BSA instead of the multiple learning strategy (denoted as MLBSA-1) and MLBSA without the elite mechanism based on chaotic local search (denoted as MLBSA-2) are tested, respectively. Table 10 gives the statistical results of MLBSA and its variants in 30 independent runs. MLBSA is clear able to get the better results than MLBSA-1 on each model in terms of all criteria, which indicates the effectiveness of the introduced multiple learning strategy. While MLBSA-2 obtains the worse results than MLBSA on each model in terms of all criteria, which demonstrates that the absence of the elite mechanism based on chaotic local search could lead to the poor search accuracy and reliability of MLBSA. In addition, Table 10 clearly shows that the integration of both multiple learning strategy and elite mechanism based on chaotic local search in MLBSA enhances the performance of the algorithm.

In summary, employing a single strategy is insufficient to obtain the desired results, but integrating them results in superior performance. This excellent performance of MLBSA verifies its appropriate balance between exploitation and exploration abilities indeed benefit from the introduced strategies in this study.

6. Conclusions and future work

This paper proposes a multiple learning backtracking search algorithm (MLBSA) to accurately and steadily identify the parameters of different PV models. In MLBSA, some individuals update their positions by leaning from the current population information and historical population information simultaneously, to enhance the population diversity and consequently improve the exploration strength of the current population. In contrast, the remaining individuals renew their positions by learning from the best individual of the current population, to improve the convergence speed and thus enhance the exploitation ability. Furthermore, the quality of current population is refined by the introduced elite strategy based on chaotic local search in each generation. Comprehensive experimental tests are conducted to investigate the performance of MLBSA on parameters identification problems of different PV models, i.e., single diode, double diode, and PV module. The experimental and statistical analyses verify the superiority of MLBSA when compared with other state-of-the-art methods in terms of accuracy, reliability, and computational efficiency. Thus, MLBSA is a promising candidate technique to solve the parameter estimation problems of photovoltaic models. Also, MLBSA can be regarded as an efficient method to solve the optimization problems in any energy and even non-energy system. It is worth noting that the computational efficiency of MLBSA may be deteriorated when solving larger or smaller systems compared with other methods.

Table 9
IAE of MLBSA on PV module model.

| Item	Measured data		Simulated current data		Simulated power data	
	V (V)	I (A)	I_{sim} (A)	IAE_I (A)	P_{sim} (W)	IAE_P (W)
1	0.1248	1.0315	1.02911916	0.00238084	0.12843407	0.00029713
2	1.8093	1.0300	1.02738107	0.00261893	1.85884058	0.00473842
3	3.3511	1.0260	1.02574180	0.00025820	3.43736334	0.00086526
4	4.7622	1.0220	1.02410715	0.00210715	4.87700309	0.01003469
5	6.0538	1.0180	1.02229180	0.00429180	6.18875013	0.02598173
6	7.2364	1.0155	1.01993068	0.00443068	7.38062638	0.03206218
7	8.3189	1.0140	1.01636311	0.00236311	8.45502304	0.01965844
8	9.3097	1.0100	1.01049615	0.00049615	9.40741602	0.00461902
9	10.2163	1.0035	1.00062897	0.00287103	10.22272574	0.02933131
10	11.0449	0.9880	0.98454838	0.00345162	10.87423838	0.03812282
11	11.8018	0.9630	0.95952168	0.00347832	11.32408291	0.04105049
12	12.4929	0.9255	0.92283882	0.00266118	11.52893307	0.03324588
13	13.1231	0.8725	0.87259966	0.00009966	11.45121263	0.00130788
14	13.6983	0.8075	0.80727426	0.00022574	11.05828504	0.00309221
15	14.2221	0.7265	0.72833648	0.00183648	10.35847422	0.02611857
16	14.6995	0.6345	0.63713800	0.00263800	9.36561002	0.03877727
17	15.1346	0.5345	0.53621306	0.00171306	8.11537022	0.02592652
18	15.5311	0.4275	0.42951132	0.00201132	6.67078333	0.03123808
19	15.8929	0.3185	0.31877448	0.00027448	5.06625097	0.00436232
20	16.2229	0.2085	0.20738951	0.00111049	3.36445922	0.01801543
21	16.5241	0.1010	0.09616717	0.00483283	1.58907596	0.07985814
22	16.7987	−0.0080	−0.00832539	0.00032539	−0.13985567	0.00546607
23	17.0499	−0.1110	−0.11093648	0.00006352	−1.89145594	0.00108296
24	17.2793	−0.2090	−0.20924727	0.00024727	−3.61564628	0.00427258
25	17.4885	−0.3030	−0.30086359	0.00213641	−5.26165284	0.03736266
Sum of IAE				0.04892367		0.51688806
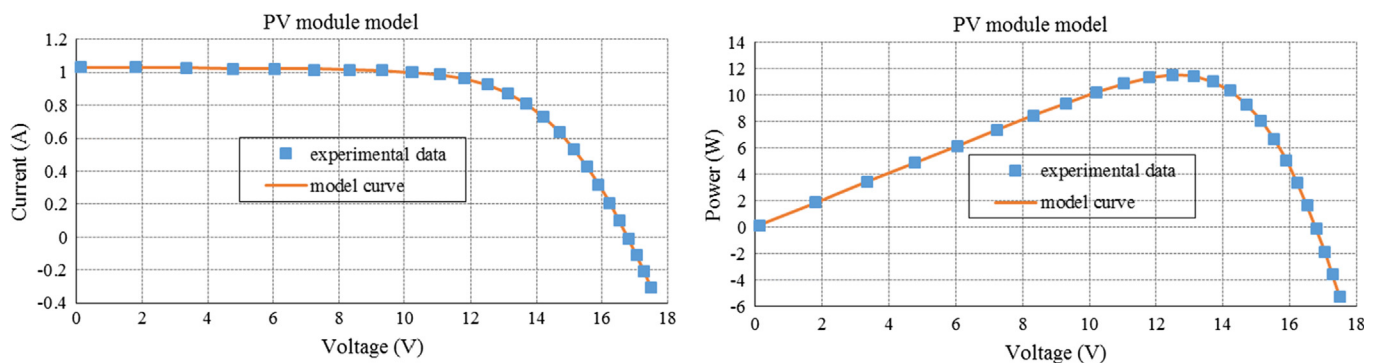
Fig. 8. Comparisons between the experimental data and simulated data obtained by MLBSA for PV module model: *I-V* and *P-V* characteristics.

Table 10
Comparisons of MLBSA with its variants for three models.

Model	Algorithm	RMSE			
		Min	Mean	Max	SD
Single diode model	MLBSA	**9.8602E-04**	**9.8602E-04**	**9.8602E-04**	**9.1461E-12**
	MLBSA-1	9.8603E-04	1.0933E-03	1.2792E-03	8.4541E-05
	MLBSA-2	**9.8602E-04**	9.8610E-04	9.8835E-04	4.2560E-07
Double diode model	MLBSA	**9.8249E-04**	**9.8518E-04**	**9.8798E-04**	**1.3482E-06**
	MLBSA-1	9.8269E-04	1.2905E-03	2.3204E-03	3.1782E-04
	MLBSA-2	9.8254E-04	9.8827E-04	1.0625E-03	1.4117E-05
PV module model	MLBSA	**2.425075E-03**	**2.425084E-03**	**2.425312E-03**	**4.336794E-08**
	MLBSA-1	**2.425075E-03**	1.148718E-02	2.742508E-01	4.962812E-02
	MLBSA-2	**2.425075E-03**	2.441645E-03	2.684042E-03	5.548312E-05

In future studies, more improvements will be made for extending the utilization of heuristic methods for complex renewable energy problems, such as energy scheduling, energy management [63,64]. The application of MLBSA for solving constrained and multi-objective optimization problems in various fields is also included in future works.

Acknowledgements

References

[1] Nunes HGG, Pombo JAN, Mariano SJPS, Calado MRA, Souza JAMFD. A new high performance method for determining the parameters of PV cells and modules based on guaranteed convergence particle swarm optimization. Appl Energy 2018;211:774–91.

[2] Gao X, Cui Y, Hu J, Xu G, Wang Z, Qu J, et al. Parameter extraction of solar cell models using improved shuffled complex evolution algorithm. Energy Convers Manage 2018;157:460–79.

[3] Muhsen DH, Ghazali AB, Khatib T, Abed IA. Parameters extraction of double diode photovoltaic module's model based on hybrid evolutionary algorithm. Energy Convers Manage 2015;105:552–61.

[4] Chin VJ, Salam Z, Ishaque K. Cell modelling and model parameters estimation techniques for photovoltaic simulator application: a review. Appl Energy 2015;154:500–19.

[5] Q. Hassan, M. Jaszczur, E. Przenzak, Mathematical model for the power generation from arbitrarily oriented photovoltaic panel, in: E3S Web of Conferences, 2017, pp. 1–10.

[6] Wu Z, Tazvinga H, Xia X. Demand side management of photovoltaic-battery hybrid system. Appl Energy 2015;148:294–304.

[7] Chen Z, Wu L, Lin P, Wu Y, Cheng S, Yan J. Parameters identification of photovoltaic models using hybrid adaptive Nelder-Mead simplex algorithm based on eagle strategy. Appl Energy 2016;182:47–57.

[8] Fathy A, Rezk H. Parameter estimation of photovoltaic system using imperialist competitive algorithm. Renew Energy 2017;111:307–20.

[9] Oliva D, El Aziz MA, Hassanien AE. Parameter estimation of photovoltaic cells using an improved chaotic whale optimization algorithm. Appl Energy 2017;200:141–54.

[10] Jordehi AR. Enhanced leader particle swarm optimisation (ELPSO): an efficient algorithm for parameter estimation of photovoltaic (PV) cells and modules. Sol Energy 2018;159:78–87.

[11] Das UK, Tey KS, Idris MYI, Mekhilef S, Seyedmahmoudian M, Horan B, et al. Forecasting of photovoltaic power generation and model optimization: a review. Renew Sustain Energy Rev 2018;81:912–28.

[12] Alam DF, Yousri DA, Eteiba MB. Flower Pollination Algorithm based solar PV parameter estimation. Energy Convers Manage 2015;101:410–22.

[13] Ma J, Ting TO, Man KL, Zhang N, Guan SU, Wong PWH. Parameter estimation of photovoltaic models via cuckoo search. J Appl Math 2013;2013:1–11.

[14] Humada AM, Hojabri M, Mekhilef S, Hamada HM. Solar cell parameters extraction based on single and double-diode models: a review. Renew Sustain Energy Rev 2016;56:494–509.

[15] Niu Q, Zhang H, Li K. An improved TLBO with elite strategy for parameters identification of PEM fuel cell and solar cell models. Int J Hydrogen Energy 2014;39:3837–54.

[16] Yu K, Chen X, Wang X, Wang Z. Parameters identification of photovoltaic models using self-adaptive teaching-learning-based optimization. Energy Convers Manage 2017;145:233–46.

[17] Easwarakhanthan T, Bottin J, Bouhouch I, Boutrit C. Nonlinear minimization algorithm for determining the solar cell parameters with microcomputers. Int J Sol Energy 1986;4:1–12.

[18] Chan DSH, Phillips JR, Phang JCH. A comparative study of extraction methods for solar cell model parameters. Solid-State Electron 1986;29:329–37.

[19] Orioli A, Di Gangi A. A procedure to calculate the five-parameter model of crystalline silicon photovoltaic modules on the basis of the tabular performance data. Appl Energy 2013;102:1160–77.

[20] Niu Q, Zhang L, Li K. A biogeography-based optimization algorithm with mutation strategies for model parameter estimation of solar and fuel cells. Energy Convers Manage 2014;86:1173–85.

[21] Ishaque K, Salam Z, Mekhilef S, Shamsudin A. Parameter extraction of solar photovoltaic modules using penalty-based differential evolution. Appl Energy 2012;99:297–308.

[22] Jiang LL, Maskell DL, Patra JC. Parameter estimation of solar cells and modules using an improved adaptive differential evolution algorithm. Appl Energy 2013;112:185–93.

[23] Askarzadeh A, Rezazadeh A. Artificial bee swarm optimization algorithm for parameters identification of solar cell models. Appl Energy 2013;102:943–9.

[24] Rajasekar N, Kumar NK, Venugopalan R. Bacterial foraging algorithm based solar PV parameter estimation. Sol Energy 2013;97:255–65.

[25] Patel SJ, Panchal AK, Kheraj V. Extraction of solar cell parameters from a single current–voltage characteristic using teaching learning based optimization algorithm. Appl Energy 2014;119:384–93.

[26] Yuan X, Xiang Y, He Y. Parameter extraction of solar cell models using mutative-scale parallel chaos optimization algorithm. Sol Energy 2014;108:238–51.

[27] Oliva D, Cuevas E, Pajares G. Parameter identification of solar cells using artificial bee colony optimization. Energy 2014;72:93–102.

[28] Askarzadeh A, Coelho LDS. Determination of photovoltaic modules parameters at different operating conditions using a novel bird mating optimizer approach. Energy Convers Manage 2015;89:608–14.

[29] Ma J, Bi Z, Ting TO, Hao S, Hao W. Comparative performance on photovoltaic model parameter identification via bio-inspired algorithms. Sol Energy 2016;132:606–16.

[30] Chen X, Yu K, Du W, Zhao W, Liu G. Parameters identification of solar cell models using generalized oppositional teaching learning based optimization. Energy 2016;99:170–80.

[31] Allam D, Yousri DA, Eteiba MB. Parameters extraction of the three diode model for the multi-crystalline solar cell/module using Moth-Flame Optimization Algorithm. Energy Convers Manage 2016;123:535–48.

[32] Awadallah MA. Variations of the bacterial foraging algorithm for the extraction of PV module parameters from nameplate data. Energy Convers Manage 2016;113:312–20.

[33] Jordehi AR. Time varying acceleration coefficients particle swarm optimisation (TVACPSO): a new optimisation algorithm for estimating parameters of PV cells and modules. Energy Convers Manage 2016;129:262–74.

[34] Lin P, Cheng S, Yeh W, Chen Z, Wu L. Parameters extraction of solar cell models using a modified simplified swarm optimization algorithm. Sol Energy 2017;144:594–603.

[35] Chen X, Xu B, Mei C, Ding Y, Li K. Teaching-learning-based artificial bee colony for solar photovoltaic parameter estimation. Appl Energy 2018;212:1578–88.

[36] Civicioglu P. Backtracking search optimization algorithm for numerical optimization problems. Appl Math Comput 2013;219:8121–44.

[37] Madasu SD, Kumar MS, Singh AK. Comparable investigation of backtracking search algorithm in automatic generation control for two area reheat interconnected thermal power system. Appl Soft Comput 2017;55:197–210.

[38] Islam NN, Hannan M, Shareef H, Mohamed A. An application of backtracking search algorithm in designing power system stabilizers for large multi-machine system. Neurocomputing 2017;237:175–84.

[39] Modiri-Delshad M, Kaboli SHA, Taslimi-Renani E, Rahim NA. Backtracking search algorithm for solving economic dispatch problems with valve-point effects and multiple fuel options. Energy 2016;116:637–49.

[40] Modiri-Delshad M, Rahim NA. Multi-objective backtracking search algorithm for economic emission dispatch problem. Appl Soft Comput 2016;40:479–94.

[41] Ayan K, Kılıç U. Optimal power flow of two-terminal HVDC systems using backtracking search algorithm. Int J Electr Power Energy Syst 2016;78:326–35.

[42] Chaib A, Bouchekara H, Mehasni R, Abido M. Optimal power flow with emission and non-smooth cost functions using backtracking search optimization algorithm. Int J Electr Power Energy Syst 2016;81:64–77.

[43] Lin J. Oppositional backtracking search optimization algorithm for parameter identification of hyperchaotic systems. Nonlinear Dyn 2015;80:209–19.

[44] Ahandani MA, Ghiasi AR, Kharrati H. Parameter identification of chaotic systems using a shuffled backtracking search optimization algorithm. Soft Comput 2017:1–23.

[45] Zhang C, Zhou J, Li C, Fu W, Peng T. A compound structure of ELM based on feature selection and parameter optimization using hybrid backtracking search algorithm for wind speed forecasting. Energy Convers Manage 2017;143:360–76.

[46] Chen D, Lu R, Zou F, Li S, Wang P. A learning and niching based backtracking search optimisation algorithm and its applications in global optimisation and ANN training. Neurocomputing 2017;266:579–94.

[47] Chen D, Zou F, Lu R, Wang P. Learning backtracking search optimisation algorithm and its application. Inf Sci 2017;376:71–94.

[48] Zou F, Chen D, Li S, Lu R, Lin M. Community detection in complex networks: multi-objective discrete backtracking search optimization algorithm with decomposition. Appl Soft Comput 2017;53:285–95.

[49] Lin J, Wang Z-J, Li X. A backtracking search hyper-heuristic for the distributed assembly flow-shop scheduling problem. Swarm Evol Comput 2017;36:124–35.

[50] Lu C, Gao L, Li X, Pan Q, Wang Q. Energy-efficient permutation flow shop scheduling problem using a hybrid multi-objective backtracking search algorithm. J Clean Prod 2017;144:228–38.

[51] Su Z, Wang H, Yao P. A hybrid backtracking search optimization algorithm for nonlinear optimal control problems with complex dynamic constraints. Neurocomputing 2016;186:182–94.

[52] Chen X, Xu B, Mei C, Ding Y, Li K. Teaching–learning–based artificial bee colony for solar photovoltaic parameter estimation. Appl Energy 2018;212:1578–88.

[53] Ram JP, Babu TS, Dragicevic T, Rajasekar N. A new hybrid bee pollinator flower pollination algorithm for solar PV parameter estimation. Energy Convers Manage 2017;135:463–76.

[54] Yu K, Wang X, Wang Z. An improved teaching-learning-based optimization algorithm for numerical and engineering optimization problems. J Intell Manuf

2016;27:831–43.

[55] Jamadi M, Merrikh-Bayat F, Bigdeli M. Very accurate parameter estimation of single-and double-diode solar cell models using a modified artificial bee colony algorithm. Int J Energy Environ Eng 2016;7:13–25.

[56] Nama S, Saha AK, Ghosh S. Improved backtracking search algorithm for pseudo dynamic active earth pressure on retaining wall supporting c-Φ backfill. Appl Soft Comput 2017;52:885–97.

[57] Zou F, Wang L, Hei X, Chen D. Teaching-learning-based optimization with learning experience of other learners and its application. Appl Soft Comput 2015;37:725–36.

[58] Liang JJ, Qin AK, Suganthan PN, Baskar S. Comprehensive learning particle swarm optimizer for global optimization of multimodal functions. IEEE Trans Evol Comput 2006;10:281–95.

[59] Chen X, Tianfield H, Mei C, Du W, Liu G. Biogeography-based learning particle swarm optimization. Soft Comput 2016:1–23.

[60] Gong WY, Cai Z, Ling CX. DE/BBO: a hybrid differential evolution with biogeo-graphy-based optimization for global numerical optimization. Soft Comput 2010;15:645–65.

[61] Chen X, Tianfield H, Du W, Liu G. Biogeography-based optimization with covar-iance matrix based migration. Appl Soft Comput 2016;45:71–85.

[62] Alcala-Fdez J, Sanchez L, Garcia S, del Jesus MJ, Ventura S, Garrell J, et al. KEEL: a software tool to assess evolutionary algorithms for data mining problems. Soft Comput 2009;13:307–18.

[63] Appino RR, Ordiano JÁG, Mikut R, Faulwasser T, Hagenmeyer V. On the use of probabilistic forecasts in scheduling of renewable energy sources coupled to storages. Appl Energy 2018;210:1207–18.

[64] Liu Z, Chen Y, Zhuo R, Jia H. Energy storage capacity optimization for autonomy microgrid considering CHP and EV scheduling. Appl Energy 2018;210:1113–25.